2.6 FOOTPRINT MODEL PERFORMANCE UNDER INHOMOGENEOUS FLOW CONDITIONS

Tiina Markkanen*
Department of micrometeorology, University of Bayreuth,
Bayreuth, Germany

G. Steinfeld
Institute of Meteorology and Climatology, Leibniz University of Hannover,
Hannover, Germany

Natascha Kljun
Department of Geography, School of the Environment and Society, Swansea University,
Swansea, UK

S. Raasch
Institute of Meteorology and Climatology, Leibniz University of Hannover,
Hannover, Germany

T. Foken
Department of micrometeorology, University of Bayreuth,
Bayreuth, Germany

1. INTRODUCTION

Footprint modeling aims at determining the areas of highest influence on concentrations or fluxes of atmospheric constituents at a certain location. This is necessary in interpreting the results of measurements, especially when those are performed over a landscape of varying surface source strengths. Varying source strength is often related to patchiness of the properties of the underlying surface, which in turn is often reflected as heterogeneity of the flow field. Contradicting these facts, however, horizontal homogeneity is a fundamental requirement of most of the existing footprint models (Foken and Leclerc 2004).

In the stochastic Lagrangian (LS) approach a large number of particles are followed as they traverse between their sources and the observation point either backward (e.g. Kljun 2002) or forward (Leclerc and Thurtel, 1990; Rannik et al., 2000) in time.

*Corresponding author address: Tiina Markkanen, University of Bayreuth, 95440 Bayreuth, Germany; e-mail: tiina.markkanen@uni-bayreuth.de

Lagrangian stochastic forward models in particular require a large number of particles for resolving local footprints under heterogeneous flow conditions. Thus they are usually used for homogeneous flow fields where the inverted plume assumption can be applied. The backward approach is more suitable for horizontally heterogeneous flow conditions, as the particles are released from unambiguous measurement position and followed towards their sources. However, it also suffers from the lack of easy description of the heterogeneous flow fields.

This problem can be overcome by pre-determining a detailed flow field with large eddy simulation (LES) which is subsequently used for Lagrangian footprint determination. This approach was used by Cai and Leclerc (2007) in both backward and forward simulations. Steinfeld et al (2008) developed a LES approach in which both turbulence statistics and turbulent dispersal of particles are calculated simultaneously. Even though this is effectively a forward approach, the method facilitates calculations for a large number of particles.

In this work we determine footprints at various heights over a surface with well defined heterogeneity in surface condition. As the

heterogeneity is given as a step change of surface properties in the surroundings of the measurement point, in the LES case this will lead to a flow pattern consisting of the component of the background wind direction and a component due to a secondary circulation driven by the heterogeneity. Thus, the local wind properties at an arbitrary observation point vary according to the distance from heterogeneity and observation height.

In this work we use the LES model PALM (Raasch and Etling, 1998; Raasch and Schröter, 2001) that has been coupled with a Lagrangian stochastic forward model for the evaluation of particle trajectories (Steinfeld et al, 2008). Furthermore, we assess the performance of Lagrangian stochastic backward footprint model (LPDM-B Kljun et al, 2002) under simple parameterization of heterogeneity.

2. MODELS

2.1 LES-model PALM

The LS particles are embedded into the LES model PALM (Raasch and Etling, 1998; Raasch and Schröter, 2001) which covers wide range boundary layer stratifications. The method for particle inclusion is based on Weil et al. (2004) where the particle velocities are separated into two parts, following the fundamental LES idea of dividing the turbulent flow field into an explicitly resolved grid scale part and a modeled sub-grid scale part. For stochastic transport Weil et al. (2004) adopted the Thomson (1987) model which assumes isotropy and Gaussianity of turbulence (see Weil et al. 2004 for more details). The grid scale flow characteristics are interpolated linearly in vertical, and bilinearly in horizontal, to sub-grid scale particle positions. Following Kim et al. (2005), no explicit boundary condition has been used at the boundary layer top.

Importantly, in the PALM embedded LS model we use, the particles are simulated online during the LES run. That is not the case in LES driven LS simulations by Weil et al. (2004), Cai et al. (2006) and Kim et al. (2005) who use precalculated LES data for separate LS simulations. The latter method is costly in terms of the disc space required, and limited by writing and reading rates of the data. Furthermore, the LES embedded LS calculations are fully parallelised which facilitates release of an exceptionally high number of particles.

A horizontal domain decomposition as used in PALM is of especially great benefit in particle dispersal simulations; this is because vertically the particles remain relatively close to each other, whereas horizontally they simultaneously cover a relatively large fraction of the domain. In fact, the particles are not expected to reach the uppermost heights of the domain at all as they are strongly bounced back at the top of the boundary layer. Thus, a vertical domain decomposition would not be as effective as the horizontal decomposition as the boundary layer parts would require much more computing time than those above. For a more detailed description of the approach see Steinfeld et al (2008).

The footprint contributions are derived according to the Kurbanmuradov et al (2000) approach for determining flux and concentration footprints from forward dispersal data. However, in the case of horizontally heterogeneous flow, instead of using all the particles crossing the measurement level, only the particles traveling through a stripe of a given width, parallel to the heterogeneity can be considered. In effect, this means that instead of providing point measurements a sensor has a horizontal dimension equal to the width of the stripe.

2.2 Backward model LPDM-B

In the LPDM-B model the dispersion is based on a model by Rotach et al (1996) and de Haan and Rotach (1998) which satisfied the well mixed condition by Thomson (1987) from convective to stable stratifications and over the whole depth of the atmospheric boundary layer. We use the model in its most parameterized form in which only surface roughness length (z_0), friction velocity (u_*), Obukhov length (L), convective velocity scale (w_*) and boundary layer height (z_i) are required as inputs. Parameterizations of mean wind speed and standard deviations are given in Rotach et al (1996). Calculation of backward trajectories and the method of deriving the flux and concentration footprints from the release and touchdown velocity data are given in Flesch et al (1995) and Flesch (1996). For a detailed description and sensitivity analysis of the model as a whole the reader is advised to examine Kljun et al (2002).

In this work, in order to consider the heterogeneity of surface properties, the dispersion domain is parameterized with data from two data sets derived from LES simulations. The two parameter sets are representative for areas at both sides of the line heterogeneity. These properties extend vertically all throughout the boundary layer and are not bent downwind as a more realistic model for internal boundary layer

development upwind from surface heterogeneity would require. Furthermore, in this simple adaptation of the LES data to the backward model wind direction is preserved even in the crossing of the heterogeneity, which is an obvious violation of conservation laws.

3. SIMULATIONS

In this work PALM is driven in its dry mode and cyclic lateral boundaries are applied. Furthermore, Monin-Obukhov similarity is applied between the surface and the first computational grid point level. Coriolis force is not considered in these simulations. Aerodynamic roughness length was set to 0.16 m. The domain, with total size 3840 m × 3840 m, was split into two equally wide parts that were driven by different surface heat fluxes (Table 1) after spin-up time of 7200 s. The mean wind in the free atmosphere was set parallel to the line dividing the two areas.

After 4 h of simulation time, altogether 14,745,600 particles were released within a half hour period. As the effective sensor sizes (i.e. widths of the stripes where particles were counted) were 20 m, 40 m and 80 m, the effective numbers used for footprint determination were 76,800, 153,600 and 307,200 respectively.

In the following discussion, the y-axis (South-North) is set parallel to the mean wind in the free atmosphere wind, thus the flow field is invariant along the y-axis.

Main split of the domain	Warm area 1920 m × 3840 m (West)	Cooler area 1920 m × 3840 m (East)
Kinematic heat flux (Kms^{-1})	0.15	0.05
u_* (ms^{-1})	0.23	0.16
w_* (ms^{-1})	1.745	0.944
z_i (m)	1094.8	527.1
L (m)	–5.59	–6.11
Further split of sub-domain acc. to flow characteristics	Nearest 460 m × 3840 m, West from dividing line	Nearest 460 m × 3840 m East from dividing line
u_* (ms^{-1})	0.237	0.177
w_* (ms^{-1})	1.329	0.913
z_i (m)	492.1	474.0
L (m)	–6.28	–7.47

Table 1: Driving parameters for LPDM-B and averages of the respective flow characteristics of sub-domains as derived from LES results. Symbols in the table are as follows: friction velocity (u_*), Obukhov length (L), convective velocity scale (w_*) and boundary layer height (z_i).

We calculated the footprints for several positions in the vicinity of the location of surface heat flux change and for positions in the middle of each half, i.e. at x = –960 m, –100 m, –50 m –10 m, 0 m, 10 m, 50 m, 100 m and 960 m. In backward model simulations the parameters for the locations within a distance of 460 m from the dividing line are given in the lower part of the Table 1, whereas the general parameters for whole domain were used for the positions x = ±960 m (Table 1 upper part).

The LES footprints were derived for heights z = 3 m, 5 m, 10 m, 20 m, 30 m, 50 m, 100 m, 200 m and 500 m. A measurement height of z_m = 30 m was selected as the basic level for comparison between LES and backward models.

4. RESULTS

4.1 Flow fields

The wind field at the height of z_m = 30 m (Figure 1) resembles those of other observation heights up to z_m = 200 m.

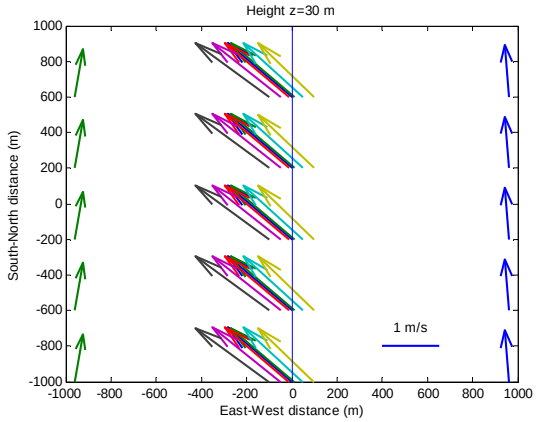

Figure 1: Wind vectors at measurement positions 960 m, 100 m, 50 m, 10 m and 0 m West and 10 m, 50 m, 100 m and 960 m East from the dividing line (colors green to blue respectively) at the observation height of 30 m. Warm surface is to West and cooler surface to East from the border between the two areas indicated with blue line.

Close to the dividing line of surface properties South-easterlies prevail close, while in the middle of each half (x = ±960 m) the winds are nearly southerlies.

At z_m = 500 m all the wind directions are close to the free atmosphere mean wind direction (Figure 2), while at yet higher levels the wind pattern turns to mirror image of that of at 30 m (Figure 1). In other words, negative values of the u-component at heights z < 500 m turn positive at

heights $z > 500$ m and vice versa (Figure not shown).

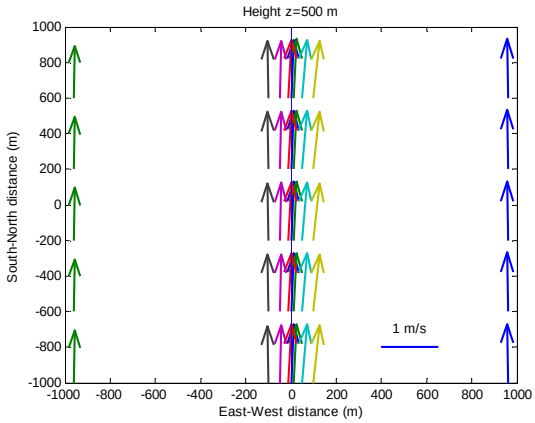

Figure 2: Wind vectors at measurement positions 960 m, 100 m, 50 m, 10 m and 0 m West and 10 m, 50 m, 100 m and 960 m East from the dividing line (colors green to blue respectively) at the observation height of 500 m. Warm surface is to West and cooler surface to East from the border between the two areas indicated with blue line.

4.2 Concentration footprints

In the following discussion the measurement position is set to origin; the y-axis is parallel to the mean wind in the free atmosphere with values growing from South to North, while the x-axis is West-East axis. LES derived concentration footprints for measurement positions 50 m West and 10 m East from the dividing line are very similar to each other (Figure 3 and 4) and consequently also very similar to positions in between including the one with measurement position directly above the change in surface properties (not shown). The most prominent footprint areas close to the peak position show high agreement both in location and width. Main difference between the two models is found in the tails of the footprints. While that of the backward model extends directly upwind according to the south-westerly wind direction at the measurement point, the LES predicted footprint turns towards South. The latter behavior is due to the heat flux pattern generated secondary circulation with southerly wind direction at distances corresponding to the location of the tail (Figure 1) and at higher levels of the boundary layer (Figure 2). This cannot be considered by the backward model which was only provided with the mean wind direction at the measurement position.

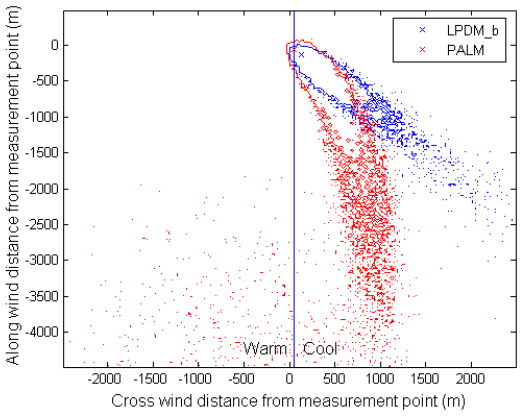

Figure 3: Concentration footprints from conventional Backward LS model LPDM-B (blue contour) and LES model PALM (red contour) at z_m = 30 m. Measurement position is at (0, 0) and the step change of surface properties (blue line) is 50 m West from the measurement position. Contours indicate the smallest areas contributing 80% of the total concentration signal (i.e. contribution from the whole domain area). Cross indicates the location of the maximum of the footprint function.

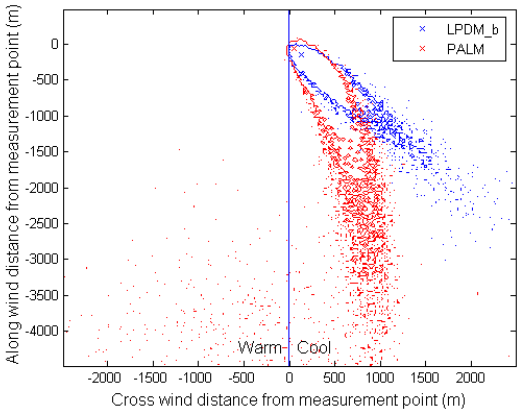

Figure 4: Concentration footprints from conventional Backward LS model LPDM-B (blue contour) and LES model PALM (red contour) at z_m = 30 m. Measurement position is at (0, 0) and the step change of surface properties (blue line) is 10 m East from the measurement position. See the figure caption of the Figure 3 for meaning of contours and crosses.

At distance 100 m West of the dividing line the central LES model derived footprint is somewhat narrower than in the previous two cases (not shown). This is a slight indication of the influence of higher heating at the Western part of the domain. At the same distance East of the dividing

line (not shown) the LES model derived footprint is very similar to those closer to the line (Figure 3 and 4).

At distance x = 960 m to East from the dividing line the concentration footprints are slightly wider in the cross wind direction than those closer to the dividing line (Figure 5). Even though the backward model LPDM-B predicts a peak position somewhat more upwind than LES model PALM does, resemblance between the predictions from both models is very close.

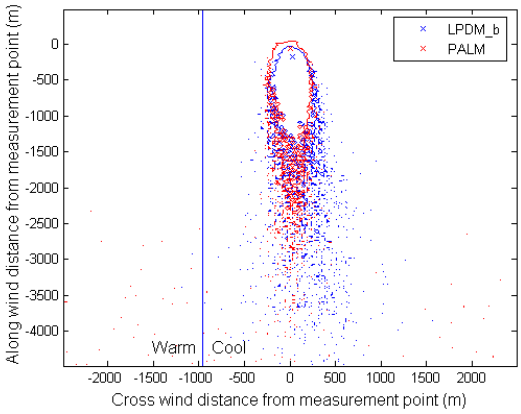

Figure 5: Concentration footprints from conventional Backward LS model LPDM-B (blue contour) and LES model PALM (red contour) at z_m = 30 m. Measurement position is at (0, 0) and the step change of surface properties (blue line) is 960 m East from the measurement position. See the figure caption of the Figure 3 for meaning of contours and crosses.

At distance x = 960 m to West from the dividing line the concentration footprints predicted by both models differ most from each other among the measurement positions studied in this work (Figure 6). While footprint predicted by the backward model is slightly wider compared to that over the cooler half of the domain (Figure 5), the footprint from LES model shows two prominent branches with tails extending first south-east and south-west and eventually bending towards south.

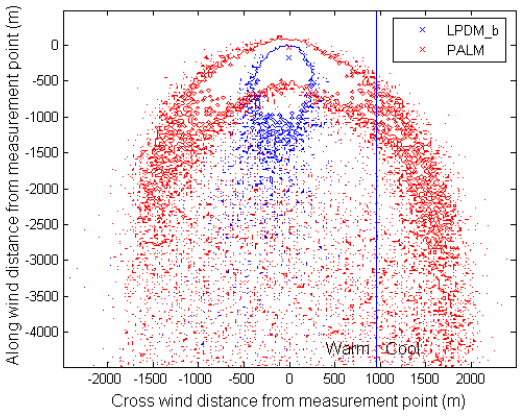

Figure 6: Concentration footprints from conventional Backward LS model LPDM-B (blue contour) and LES model PALM (red contour) at z_m = 30 m. Measurement position is at (0, 0) and the step change of surface properties (blue line) is 960 m West from the measurement position. See the figure caption of the Figure 3 for meaning of contours and crosses.

4.3 Flux footprints

PALM predicts larger concentration footprint areas of 80% of the signal than LPDM-B does, whereas the flux footprints for the observation positions in the middle of the domain show opposite behavior. For observation point 50 m West from the dividing line (Figure 7) the flux footprint predictions by both models are of approximately same width. However, the LES derived footprint has its maximum very close to the measurement position and its most prominent part fades off within 200 m from the maximum. This is due to the secondary circulation bringing to the area descending particles which cancel out the positive contribution of ascending particles to the flux. The tail of the flux footprint, even though of relative low contribution to the flux, is similarly positioned as that of the corresponding concentration footprint (Figure 3) As the simple parameterization of wind direction is used in LPDM-B, it extends according to mean wind at the measurement point.

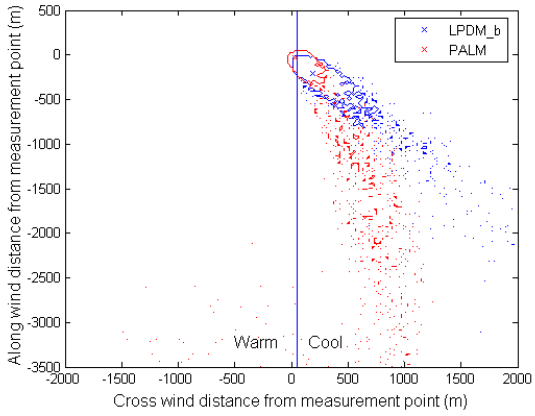

Figure 7: Flux footprints from conventional Backward LS model LPDM-B (blue contour) and LES model PALM (red contour) at z_m = 30 m. Measurement position is at (0, 0) and the step change of surface properties (blue line) is 50 m West from the measurement position. Contours indicate the smallest areas contributing 80% of the total positive flux signal (i.e. sum of positive contribution from the whole domain area. The areas of negative flux footprint due to secondary circulation are neglected). Cross indicates the location of the maximum of the footprint function.

At measurement position 960 m East from the dividing line the fading off the tail of the LES predicted footprint is more pronounced than in the previous case. Otherwise the footprints predicted by both models are very symmetrical across the mean wind direction and of approximately same widths.

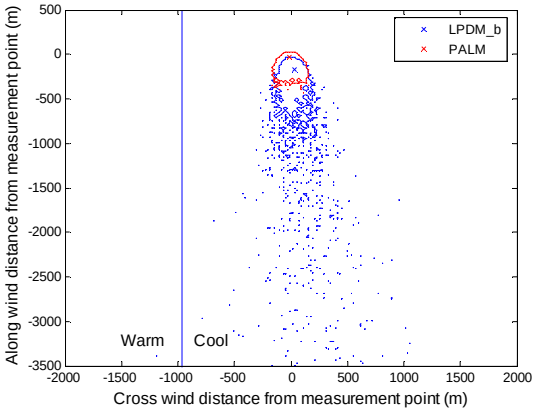

Figure 8: Flux footprints from conventional Backward LS model LPDM-B (blue contour) and LES model PALM (red contour) at z_m = 30 m. Measurement position is at (0, 0) and the step change of surface properties (blue line) is 960 m East from the measurement position. See the figure caption of the Figure 7. for meaning of contours and crosses.

At the position of 960 m West from the dividing line the flux footprints (Figure 9) show close resemblance to the respective concentration footprints (Figure 6). The LES predicted footprint consists of a wide central part with two tails bending South at both sides. Pronounced fading off by descending particles is not observed here, which is due to positive mean vertical winds over the warm surface.

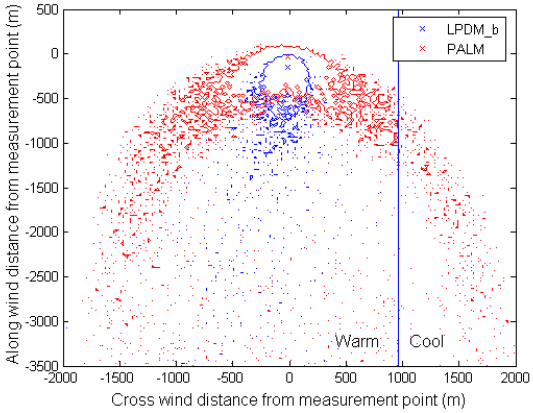

Figure 9: Flux footprints from conventional Backward LS model LPDM-B (blue contour) and LES model PALM (red contour) at z_m = 30 m. Measurement position is at (0, 0) and the step change of surface properties (blue line) is 960 m West from the measurement position. See the figure caption of the Figure 7 for meaning of contours and crosses.

5. CONCLUSIONS

This work aimed at studying the applicability of a conventional backward LS model with a highly simplified parameterization of heterogeneity under flow conditions characterized by a secondary circulation. The flux and concentration footprints predicted by the two models used in the study – the LES model PALM embedded particle dispersion model and backward LS model LPDM-B – seemed to agree well for the most prominent parts of the footprint areas. Around the peak position which indicates the location of most importance to the signals the two footprint predictions were generally of similar width and shape. In all of the cases studied the LES model predicted peak positions closer to the measurement point than backward LS model LPDM-B. The concentration footprints, especially, showed high resemblance except for the tails of the areas accounting for 80% of the total signals from within the domain of 3840 m × 3840 m. The

influence of secondary circulation is of higher importance in the case of flux footprints as descending particles reduce the contribution of their rising companions at some areas of the domain in the LES predictions.

All in all, we conclude that traditional backward LS model mostly perform well in footprint predictions even with simple parameterization of flow conditions except for most pathological flow patterns with pronounced secondary circulations. Concerning routine use of footprint models a question arises, how to recognize such conditions under which special caution has to be taken.

ACKNOWLEDGEMENTS

The project was funded by the German Science Foundation under the contracts FO 226/10-1, 2 and RA 617/16-1, 2 and by ETH, Zürich.

REFERENCES

Cai, X.H., and M.Y. Leclerc, 2007: Forward-in-time and backward-in-time dispersion in the convective boundary layer: The concentration footprint. *Boundary-Layer Meteorol,* **123**, 201-218.

Cai, X.H., R. Zhang and Y. Li, 2006: A large-eddy simulation and Lagrangian stochastic study of heavy particle dispersion in the convective boundary layer. *Boundary-Layer Meteorol.,* **120**, 413-435.

de Haan, P., and M.W. Rotach, 1998: A novel approach to atmospheric dispersion modelling: the Puff-particle model (PPM). *Quart. J. Roy. Meteorol. Soc.,* **124**, 2771–2792.

Flesch, T.K., 1996: The footprint for flux measurements, from backward Lagrangian stochastic models. *Boundary-Layer Meteorol*., **78**, 399–404.

Flesch, T.K., J.D. Wilson and E. Yee, 1995: Backward-time Lagrangian stochastic dispersion models and their application to estimate gaseous emissions. *J. Appl. Meteorol.,* **34**, 1320–1332.

Foken, T., and M.Y. Leclerc, 2004: Methods and limitations in validation of footprint models. *Agricultural and Forest Meteorology*, **127**, 223–234.

Kim S.W., C.H. Moeng, J.C. Weil and M.C. Barth, 2005: Lagrangian particle dispersion modeling of the fumigation process using large-eddy simulation. *J. Atmos. Sci.,* **62**, 1932-1946.

Kljun, N., P. Kastner-Klein, E. Fedorovich and M.W. Rotach, 2004: Evaluation of Lagrangian footprint model using data from wind tunnel convective boundary layer. *Agricultural and Forest Meteorology,* **127**, 189–201.

Kljun, N., M. W. Rotach and H.P. Schmid, 2002: A three-dimensional backward Langrangian footprint model for a wide range of boundary-layer stratifications. *Boundary-Layer Meteorol.,* **103**, 205–226.

Kurbanmuradov O., and Ü. Rannik, K.K. Sabelfeld and T. Vesala, 2001: Evaluation of mean concentration and fluxes in turbulent flows by Lagrangian stochastic models. *Mathematics and Computers in Simulation*, **54**, 459-476.

Leclerc, M.Y., and G.W. Thurtell, 1990: Footprint prediction of scalar fluxes using a Markovian analysis. *Boundary-Layer Meteorol.,* **52**, 247–258.

Raasch, S., and D. Etling, 1991: Numerical simulations of rotating turbulent thermal convection. *Beitr. Phys. Atmos.,* **64**, 185–199.

Raasch, S., and M. Schröter, 2001: PALM – a large-eddy simulation model performing on massively parallel computers. *Meteorol. Z.*, **10**, 363–372.

Rannik, Ü., M. Aubinet, O. Kurbanmuradov, K.K. Sabelfeld, T. Markkanen and T. Vesala, 2000: Footprint Analysis for Measurements over a Heterogeneous Forest. *Boundary-Layer Meteorol.,* **97**, 137–166.

Rotach, M.W., S.-E. Gryning and C. Tassone, 1996: A two-dimensional Lagrangian stochastic dispersion model for daytime conditions. *Quart. J. Roy. Meteorol. Soc.,* **122**, 367–389.

Steinfeld, G., S. Raasch and T. Markkanen, 2008: Evaluation of footprints in homogeneous and inhomogeneous terrain with a Lagrangian stochastic particle model embedded into a large eddy simulation model, *Boundary-Layer Meteorol.,* under review

Thomson, D.J., 1987: Criteria for the selection of stochastic models of particle trajectories in turbulent flows. *Journal of Fluid Mechanics*, **180**, 529-556.

Weil J.C., P.P. Sullivan and C.H. Moeng, 2004: The use of large-eddy simulations in Lagrangian particle dispersion models. *J. Atmos. Sci.,* **61**, 2877-2887.